

## Comparison of periodic light-trapping structures in thin InGaN-based solar cell

A. Merabti <sup>a,b,\*</sup>, R. Abdeldjebar <sup>a</sup>, S. Nour <sup>a,b</sup>, H. Aissani <sup>a,b</sup>, A. A. Djatout <sup>a</sup>

<sup>a</sup> *Exact Sciences, Higher Normal School of Béchar, Algeria*

<sup>b</sup> *Semiconductor Devices Physics Laboratory, University Tahri Mohammed Béchar, Algeria*

This study presents a theoretical analysis of light-trapping efficiency in thin-film InGaN solar cells by examining four distinct one-dimensional periodic surface structures: a proposed geometric model [1], pyramid, trapezium, and triangle with two curved. Utilizing the Finite Element Method (FEM), we systematically analyze the optical absorption characteristics for various grating configurations with fixed structural parameters. Our results reveal that the proposed geometric model offers enhanced broadband absorption across the visible spectrum and maintains superior performance over a wide range of incidence angles, indicating strong potential for photovoltaic applications.

(Received April 21, 2025; Accepted July 3, 2025)

**Keywords:** Thin-film, Grating structure, Absorption, InGaN, Light trapping

### 1. Introduction

The phenomenon of light trapping in InGaN is one of modern optical events that draws a great deal of attention to the area of optoelectronics and advanced energy applications. InGaN is characterized by its unique ability to trap the photons in the crystalline structure, due to the high refraction index and extraordinary optical properties [2]. As a result, it emerges as an outstanding contender for enhancing light absorption in both solar cells and LEDs [3-4]. When nanostructure or hasty patterns are constructed on the surface of the interior, the interaction between light and materials can be greatly increased. This increased interaction improves photon absorption efficiency, especially on the wavelength near the band gap, open new lanes to adapt to opto-electronic devices. In addition, the ability to set the indium composition in the engagement allows better compliance with the sun spectrum, which increases the efficiency of produced solar cells. Thanks to these properties, InGaN is considered a promising platform to develop a new generation of opto-electronic units.

In addition to their tunable band gap, InGaN materials, better radiation stiffness, high charged carrier mobility and a remarkably large absorption coefficients, and a significantly large absorption coefficients, all of which increase their ability to high deficit photovoltaic applications [5]. These properties not only make InGaN a strong candidate to operate in a stiff environment, such as space, but also efficient light harvesting and charging transport, which are important for adapting to the performance of the next generation of solar systems in the next generation.

Indium gallium nitride, or InGaN, has really piqued interest in the world of solar technology— and for good reason! Its remarkable optoelectronic characteristics are simply fascinating. Picture this: a meticulously adjustable direct band gap that spans [6], from 0.7 eV (when it's InN) all the way up to a striking 3.4 eV (that's GaN for you)! This feature empowers it to efficiently capture a wide array of solar radiation, making it a true game-changer in solar fabrication [7-8]. Recent studies have shown that InGaN-based solar cells can also get high performance on ultra-thickness, usually in the range of 200-400 nm, due to their high absorption coefficients [9]. It is significantly thinner than traditional silicone -based solar cells, requiring a thickness of 150-200  $\mu\text{m}$  to achieve comparable absorption [10-11]. Opting for low-content materials not only slashes production costs but also enhances versatility, making them ideal for nimble and adaptable

---

\* Corresponding author: merabti73@yahoo.com

<https://doi.org/10.15251/JOR.2025.214.399>

photovoltaic applications. The advancements in epitaxial growth methods—like metal-organic chemical vapor deposition (MOCVD) and molecular beam epitaxy (MBE)—have paved the way for creating high-quality InGaN thin films, all while keeping defects to an absolute minimum [10-13]. In addition, the integration of InGaN into Multi-Junction architecture has shown a promise to achieve power conversion capacity beyond the Shockley-Queisser area by adapting photon management and carrier extraction. Despite the challenges such as false discrepancies and the doping efficiency of the p-type, the ongoing research in nanostructuring and bandgap Engineering has continued the limits of the next generation-based solar cells for photovoltaic technologies.

Traditional light trapping strategies in solar cells vary greatly depending on material and cell architecture. Indium gallium nitride-based solar cells, light handling are especially important due to their ultrathin layers, usually from 200 to 400 nm. Unlike silicon-based cells, which depend on pyramidal or random texture to get trapping, InGaN solar cells often use advanced nanostructuring techniques to increase photon absorption and carrier generation. For example, photonic crystals are effectively appeared in the thin inside layer to limit light, which improves absorption efficiency. These nanostructures not only reduce the reflection deficit, but also enable broadband light capture in visible and close range, which is necessary to maximize the performance of InGaN's tunable bandgap. In addition, the integration of transparent leading oxide (TCO) with engineering surface texture is detected to move in the InGaN layer to increase light spreading and coupling. Unlike traditional silicon slices, which require specific crystal orientation (eg [100] for pyramid structure), the flexibility of InGaN in epitaxial growth for versatile light catch design on different substrates, including sapphire and silicon [8-12]. Despite these benefits, challenges such as defective density and material quality remain important research areas to fully feel the ability of ingredient -based solar cells for high -efficiency photovoltaic applications.

In this study, we dive deep into simulations to unravel how the unique shape of specific unit cells influences light trapping in four distinct mono-periodic diffractive structures. These intriguing structures feature a variety of geometric designs, including pyramids, trapeziums, and triangles with two curved. Each shape presents a fascinating opportunity to explore how geometry affects our ability to capture and manipulate light. According to the reference [1], the suggested model for enhancing the light absorption of InGaN-based solar cells was thoroughly examined and verified by extensive simulations. There's something quite fascinating about delving into the light trapping potential nestled within various periodic structures, each with its own unique geometry. In this discussion, we're excited to present a comprehensive side-by-side comparison of all these intriguing structures. This approach enables us to make meaningful evaluations across the board. Moreover, we dive deeper by examining these structures not just at straightforward, normal angles, but also at oblique angles of incidence. This aspect is particularly crucial when considering the real-world scenarios faced by non-tracking solar cells outdoors.

In this paper, the effects of grating sizes and their assembly forms on the light-trapping ability of solar cells are studied through numerical computation using the Finite element method (FEM) to study the spectral properties of InGaN grating structures with different dimensions.

## 2. Design and modeling of the grating structure

All of the simulations in this study were run at 300 K with 1000 W/m<sup>2</sup> of incident solar radiation (AM 1.5G). The suggested gadget is a straightforward, practically thick, three-layered p-InGaN/p-InGaN/n-InGaN (PPN) solar cell. The bottom layer is an n-InGaN plane, while the top and middle layers, which are both composed of p-InGaN, have distinct indium mole fractions ( $x = 0.65$  and  $0.75$ , respectively). Interestingly, the indium mole fraction ( $x = 0.65$ ) is the same for the final n-InGaN layer and the second p-InGaN layer [1].

Four distinct mono-periodic structures have been numerically examined by us. The suggested geometric models for the structures are a trapezium, pyramid, and two-curved triangle. Figure 1 displays each structure's unit cells.

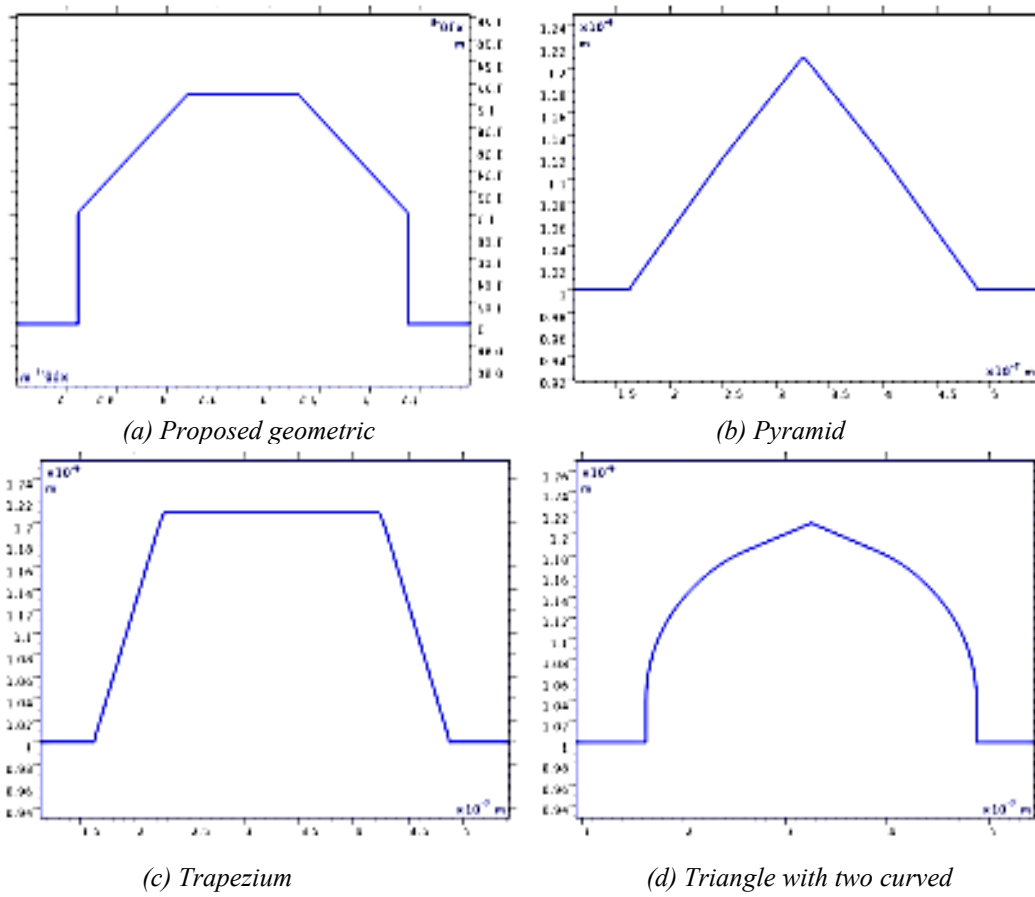


Fig. 1. The unit cell geometry of every periodic light-trapping structure under investigation.

The TE polarization's structural parameters Figure 2 shows a planar p-InGaN/p-InGaN/n-InGaN (PPN) thin film configuration with an InGaN grating structure intended to function at a wavelength of 420 nm. To optimize absorption in the active region, the top p-InGaN layer's thickness was adjusted.

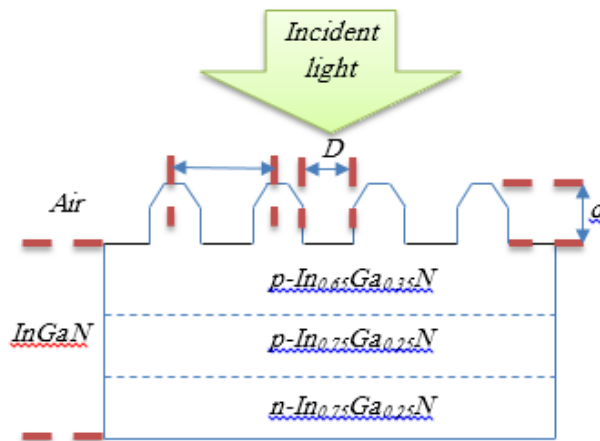


Fig 2. InGaN grating structure schematic.  $D$  is the grating width,  $d$  is the grating depth, and  $a$  is the grating period [1].

Finite Element Method (FEM) simulation software was used to examine the electric fields and absorption properties of the InGaN grating structure. The front surface of the suggested device was illuminated by incident plane waves with free-space wavelengths between 350 and 750 nm in these simulations. This study will serve as a foundational reference for a comparative analysis with three geometric shapes: a pyramid, a triangle with two curved faces, and a trapezium. The simulation methodology will remain consistent with the reference study, utilizing the same layered structure (p-InGaN/p-InGaN/n-InGaN) and material properties. However, the geometric configuration of the top surface will be altered to explore the light-trapping efficiency and absorption enhancement in each of the three shapes. By comparing the performance of pyramid, trapezium, and triangle with two curved geometries, we aim to identify the most effective design for maximizing light absorption in the solar cell's active area.

In order to maintain consistency with the previously proposed model, we will adopt the same dimensions (like period, height, and width) that were optimized in the earlier study. These dimensions were determined using TE-polarized light, which was also employed in our current simulations. The InGaN material's bandgap energy ( $E_g$ ), which is a function of the indium content ( $x$ ) in  $\text{In}_x\text{Ga}_{1-x}\text{N}$ , determines the real and imaginary components of its refractive indices. The following equation [14–15] expresses this relationship:

$$n(h\nu) = \sqrt{a(x) \left( \frac{h\nu}{E_g} \right)^{-2} \left[ 2 - \left( 1 + \sqrt{\frac{h\nu}{E_g}} - \left( 1 - \sqrt{\frac{h\nu}{E_g}} \right) \right) \right]} + b(x) \quad (1)$$

where  $a(x)$  and  $b(x)$  are fitting parameters,  $h$  is Planck's constant,  $n$  is the laser emission frequency, and  $E_g$  is the material's band gap.

The equation given in the cited study yields the fitting parameters  $a(x)$  and  $b(x)$ , which are obtained from spectrally resolved refractive index measurements of the binary compounds (GaN, AlN, and InN).

$$a(x) = 13.55x + 9.31(1 - x) \quad (2)$$

$$b(x) = 2.05x + 3.03(1 - x) \quad (3)$$

Even though Peng's approach uses more experimental refractive index data than Bergmann and Casey's, it still has some inconsistencies that are comparable to those found in their work [16–18]. These limitations highlight the need for careful consideration when applying these models to ensure accurate simulations and reliable results.

In this study, rather than optimizing the dimensions again, we will use the previously determined dimensions to compare the light-trapping efficiency and absorption characteristics of three geometric shapes: the pyramid, trapezium, and triangle with two curved. By maintaining the same structural parameters and material properties, we aim to isolate the impact of geometric variation on the device's performance. This approach will allow us to systematically evaluate which of the three shapes offers the most effective light absorption and overall enhancement in the solar cell's efficiency.

### 3. Results and discussion

#### 3.1. Light trapping at normal incidence

Plots depicts the absorption as a function of wavelength in the range of 300 nm from 400 nm to 700 nm Figure 3. Each curve corresponds to the absorption properties of separate geometric configurations: pyramids, trapesoids, triangles with two curved sides and proposed model.

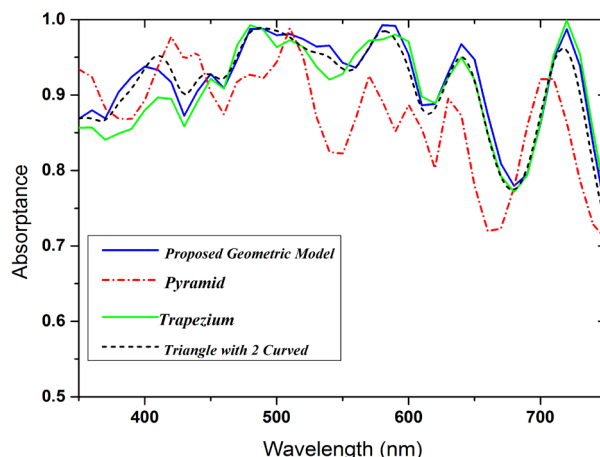


Fig. 3. Absorptance spectra of geometric models: pyramid, trapezium, triangle with two curved sides, and proposed model across the visible spectrum.

The pyramidal model is known for its ability to reduce reflection and enhance light trapping, especially at shorter wavelengths (from 400 nm to 500 nm). In this range, smaller structures (such as pyramids) are more effective due to the interaction of blue and violet light with the fine structures). If the proposed curve shows a higher absorptance than the pyramid, it indicates that the proposed model includes additional improvements to enhance performance. The trapezoidal structure exhibits intermediate absorptance with potential peaks at specific wavelengths (from 500 nm to 600 nm). In this range, medium-sized structures (such as trapezoids) are more effective at absorbing green and yellow light). In comparison, the proposed curve shows more stable absorptance across a wider range, indicating a more optimized design. The triangle with two curved sides: It exhibits high absorptance at specific wavelengths due to its curved features (550 nm to 650 nm). In this range, larger structures (such as a triangle with two curved sides) are more effective at absorbing red light. However, the proposed curve outperforms it by either broadening the absorptance range or enhancing peak performance through advanced geometric tuning.

Finally, the proposed model curve shows high absorption from visible range (between 400 nm to 700 nm), suggesting that the suggested model is highly efficient at capturing light at a variety of wavelengths. The curve also shows specific peaks at some wavelength, indicating that the proposed structure is adapted to maximum absorption on these points, due to better light catch mechanisms and advanced surface function design.

### 3.2. Absorptance behavior of geometric models under different incident angles

The optical spectra of the four distinct mono-periodic structures are displayed in Figure 4. In trapezoidal shapes, reflectivity notably rises as the angle of incidence increases. It begins around 0.1 at an angle of 40 degrees and climbs to nearly 0.9 at 80 degrees. This rise happens because the critical angles lead to total reflection and because the slanted surfaces help reflect light more effectively. Regarding transmittance, it declines as the incidence angle grows, starting from about 0.7 at 40 degrees and falling to roughly 0.1 at 80 degrees. This decline is attributed to greater amounts of reflection and scattering occurring at the angled surfaces. Absorption stays mostly steady with a slight rise, fluctuating between 0.2 and 0.4 as the incidence angle increases, which suggests that the material takes in a moderate level of light, particularly at higher angles where light travels further within the material.

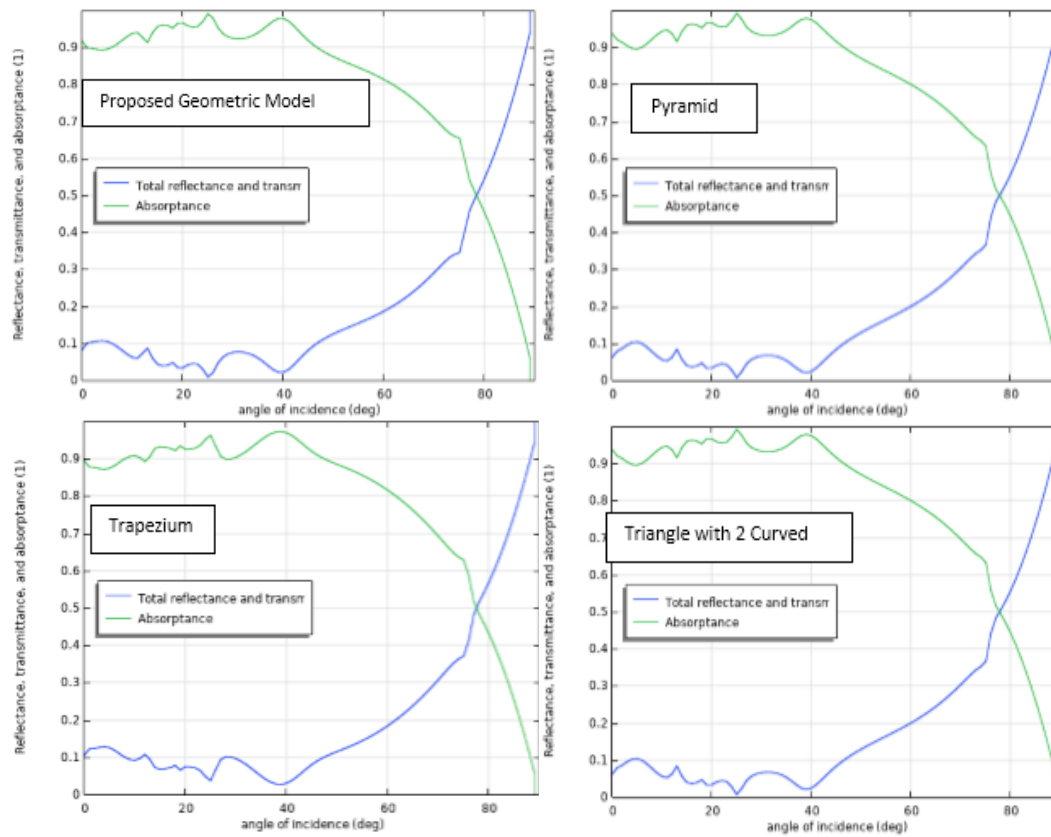


Fig. 4. Absorptance performance of geometric models: pyramid, trapezium, triangle with two curved sides, and proposed model across incident angles.

For a triangular shape that has two curved surfaces, we see a similar pattern where reflectivity increases with a higher angle of incidence, beginning around 0.1 at an angle of 40 degrees and reaching about 0.9 at 80 degrees. The curves of the faces lead to more light scattering, which enhances reflection at larger angles. As the incidence angle rises, transmittance drops, starting from about 0.7 at 40 degrees and reducing to approximately 0.1 at 80 degrees, influenced by the increased reflection and scattering on the curved surfaces. The absorption value varies between 0.2 and 0.4, which also rises slightly with a higher angle due to curvature causing light to travel longer paths within the material.

In the case of the pyramid, the reflectivity again shows a significant increase with rising incidence angles, starting at roughly 0.1 at a 40-degree angle and increasing to about 0.9 at 80 degrees. The slanted sides of the pyramid contribute to stronger reflection at larger angles. Similarly, as the incidence angle grows, transmittance decreases from around 0.7 at a 40-degree angle down to about 0.1 at 80 degrees due to enhanced reflection and scattering on the angled surfaces. Absorption remains between 0.2 and 0.4 as the incidence angle rises, with the inclination of the surfaces causing a slight uptick in absorption as light travels a longer route through the material.

In the geometry we have proposed, there is a noticeable rise in reflectivity with an increasing angle of incidence. It starts at roughly 0.1 with a 40-degree angle and climbs to about 0.9 at an 80-degree angle. The transmittance shows a downward trend as the incidence angle rises, beginning at approximately 0.7 at 40 degrees and dropping to about 0.1 at 80 degrees due to higher reflection and absorption rates. Absorption is recorded between 0.2 and 0.4 with escalating incidence angles, displaying a minor increase at larger angles as light takes a longer journey through the material.

Based on the four previous analyses, we observe that all the geometric figures including the trapezium, the triangle with two curved surfaces, the pyramid, and the suggested shape show similar patterns regarding how they reflect and transmit light. As the angle of incidence increases,

reflectivity goes up while transmittance goes down. Nonetheless, the suggested shape demonstrates slightly greater values of absorptivity at larger angles, reaching about 0.4, in contrast to the 0.2-0.3 values of the other forms. Consequently, we can say that the suggested shape is the best option for absorption, particularly at higher angles, as it captures more light than the other shapes.

### 3.3. Electric field distribution in various structures for enhanced light confinement

Light confinement in InGaN relies on the material's ability to concentrate the electric field in specific regions, enhancing the interaction between light and matter. The figure.5 show the distribution of electric field intensity over a surface at a wavelength of 580 nm, where the horizontal axis represents the distance in meters (m), and the vertical axis represents the electric field intensity in volts per meter (V/m) for studied models: proposed geometric model, pyramid, trapezium, and triangle with two curved. We will focus our analysis on the models and neglect the upper air region. The electric field intensity values are also shown on a color scale, with hotter colors (such as red) indicating higher intensity, while cooler colors (such as blue) indicate lower intensity.

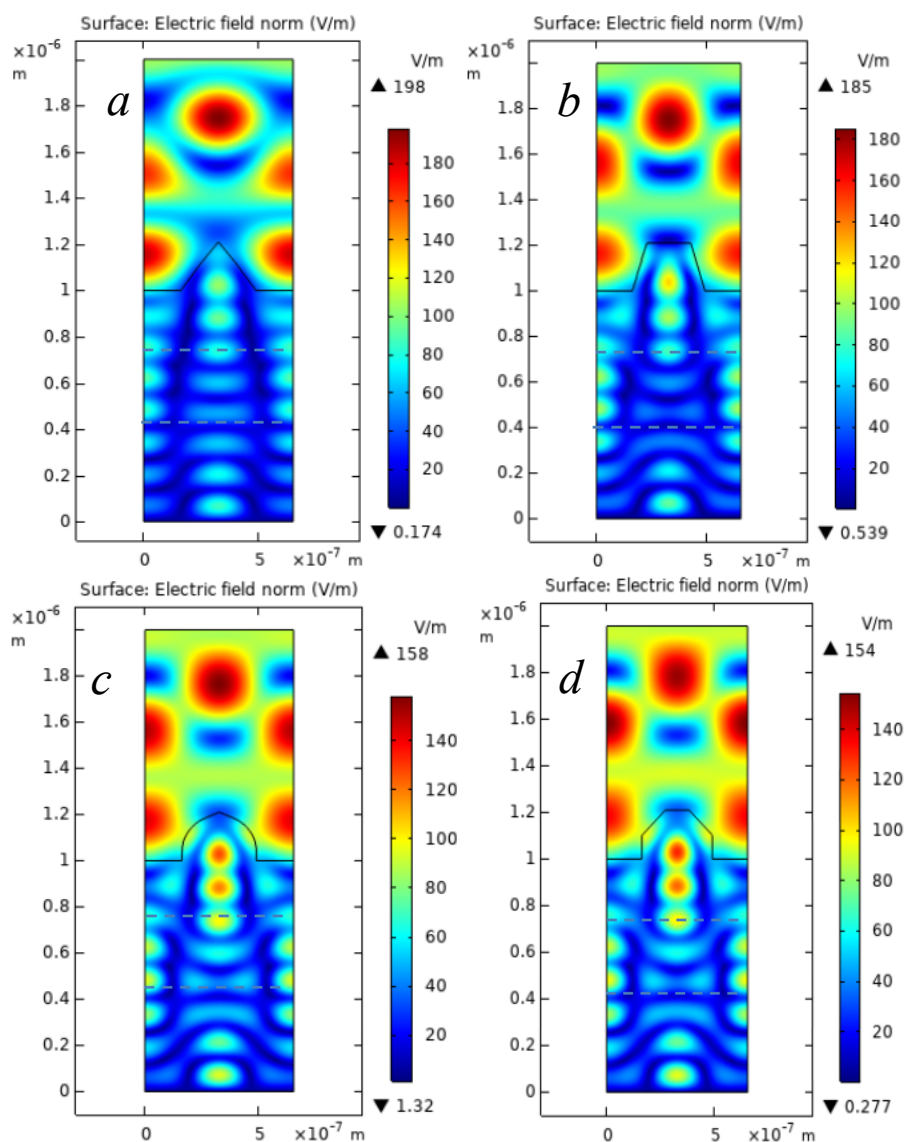


Fig. 5. Electric field intensity distribution at 580 nm wavelength for: a) pyramid, b) trapezoid, c) triangle with two curved sides, and d) proposed geometric structure.

In a simulated pyramid-shaped model, electric field strength values range from 0.174 to 100 V/m. Regions of medium intensity (around 100 V/m) appear within the pyramid, indicating a medium electric field concentration in that region. Other regions of low intensity (around 0.174 V/m) indicate a weak electric field. The pyramidal model exhibits a low electric field concentration throughout most of the model. The medium electric field concentration at the top and edges may be due to the tip enhancement effect, a well-known phenomenon in nanostructures where electric charges are concentrated in sharp regions.

When we examine the trapezium model, the image shows an average concentration of the electric field inside the trapezium and its edges, indicating that the trapezium shape acts to confine light or enhance the electric field in these regions. This average concentration of the electric field results from the fact that the electric field is more uniform near the edges of the obtuse angles. The electric field intensity values range from 0.539 to 118 V/m. It is also noticeable that the electric field distribution is heterogeneous, with regions of average concentration (especially in the interior and edges) and low concentrations.

for triangle with two curved sides, the power value of the the electric field strength values range from 1.32 to 120 V/m, in the presence of high intensity areas around 120 V/m inside the triangle and in the curved regions, indicating a strong concentration of the electric field in those regions. This indicates that the shape acts to confine light or enhance the electric field in these regions, perhaps due to the effect of sharp corners and curves (Edge and Curvature Enhancement Effect), where electric charges are concentrated in the sharp and curved regions. There are other regions with low intensity around 1.32 V/m, indicating a weak electric field in them. It shows a strong concentration of the electric field inside the pattern and in the curved regions.

The proposed model: From the picture, it can be seen that the electric field strength values within the model range from 0 to 130 V/m. High intensity regions around 130 V/m are visible, indicating a strong electric field concentration in those areas. Concurrently, there are other regions with a low intensity around 0.277 V/m, indicating a weak electric field. Note that the electric field distribution is almost homogeneous, with regions of high and low concentration.

The proposed model succeeded in confining light within the model and at all its edges. This is due to the geometric design of the model (such as corners and curves), which concentrates the light, meaning the electric field lines are concentrated, leading to increased field strength in those regions. This is known as the Edge Enhancement Effect.

#### 4. Conclusion

Four distinct periodic structures with fundamentally different unit cell geometry have had their light-trapping potentials optimized and compared. These include the proposed geometric model [1], pyramids, trapezium, and triangle with two curved sides. The proposed geometric model represents a highly optimized geometric model that outperforms the pyramid, trapezium, and triangle with two curved sides in terms of absorptance across the visible spectrum. Furthermore, the analysis of the four geometric shapes reveals that all exhibit increased reflectance and decreased transmittance with higher angles of incidence, with absorptance ranging between 0.2 and 0.4. However, the proposed geometric shape demonstrates the highest absorptance values (approximately 0.4) at larger angles. Additionally, The proposed model also features light confinement and electric field enhancement (up to 130 V/m) thanks to its geometric focusing and tip enhancement effects.

Its design likely incorporates advanced features that enhance light trapping and minimize reflection, making it a promising candidate for applications in optics and photonics. Experimental validation and further refinement of this model could lead to significant advancements in energy-efficient optical devices.

This integrated analysis highlights the importance of geometric design in optimizing light absorption and distinguishes the proposed model as a superior solution for practical applications.



## Acknowledgments

The University Training Research Project PRFU-2022 (Grant Nos. B00L02EN080120220001) provided funding for this work. The Semiconductor Devices Physics Laboratory's assistance is also valued by the authors.

## References

- [1] A. Merabti, H. Aissani, S. Nour, R. Abdeldjebar, A.A. Djatout, Journal of Ovonic Research Vol. 18, No. 6, November - December 2022, p. 753 – 758; <https://doi.org/10.15251/JOR.2022.186.753>
- [2] L. Hsu, W. Walukiewicz, J. Appl. Phys. 104 (2008) 1-7; <https://doi.org/10.1063/1.2952031>
- [3] Griffiths, A.D.; Herrnsdorf, J.; McKendry, J.J.D.; Strain, M.J.; Dawson, M.D. Philos. Trans. R. Soc. A Math. Phys. Eng. Sci. 2020, 378, 20190185; <https://doi.org/10.1098/rsta.2019.0185>
- [4] Yu, L.; Wang, L.; Hao, Z.; Luo, Y.; Sun, C.; Xiong, B.; Han, Y.; Wang, J.; Li, H., Semicond. Sci. Technol. 2022, 37, 023001; <https://doi.org/10.1088/1361-6641/ac40ec>
- [5] Ashraful Ghani Bhuiyan, Kenichi Sugita, Akihiro Hashimoto, A. Yamamoto, IEEE J Photovoltaics 2 (2012) 276 -293; <https://doi.org/10.1109/JPHOTOV.2012.2193384>
- [6] N. Annab, T. Baghdadli, S. Mamoun, A. E. Merad. Journal of Ovonic Research Vol.19, No. 4, July - August 2023, p. 421 – 431; <https://doi.org/10.15251/JOR.2023.194.421>
- [7] H.U. Manzoor, M.A.M. Zawawi, M.Z. Pakhuruddin, S.S. Ng, Z. Hassan, Phys. B Condens. Matter. 622 (2021); <https://doi.org/10.1016/j.physb.2021.413339>
- [8] T.H. Anderson, A. Lakhtakia, P.B. Monk, J. Photonics Energy. 8 (2018) 1- 17; <https://doi.org/10.1117/1.JPE.8.034501>
- [9] L. Redaelli; A. Mukhtarova; S. Valdueza-Felip; A. Ajay; C. Bougerol; C. Himwas; J. Faure-Vincent; C. Durand; J. Eymery; E. Monroy. Effect of the quantum well thickness on the performance of InGaN photovoltaic cells. Volume 105, Issue 13;29 September 2014; <https://doi.org/10.1063/1.4896679>
- [10] K. Prabakaran, R. Ramesh, P. Arivazhagan, M. Jayasakthi, S. Sanjay, S. Surender, S. Pradeep, M. Balaji, K. Baskar, J. Alloys Compd. 811 (2019) 151803; <https://doi.org/10.1016/j.jallcom.2019.151803>
- [11] Li Liang and al., Chin. Phys. B Vol. 22, No. 6 (2013) 068802; <https://doi.org/10.1088/1674-1056/22/6/068802>
- [12] K. Khan, M. Biswas, E. Ahmadi, AIP Adv. 075120 (2020) 6; <https://doi.org/10.1063/5.0012854>
- [13] O.K. Jani, Development of wide-band gap InGaN solar cells for high-efficiency photovoltaics, Georgia Institute of Technology, 2008.
- [14] Laws GM, Larkins EC, Harrison I, Molloy C, Somerford D., J Appl Phys. 2001;89:1108-1115; <https://doi.org/10.1063/1.1320007>
- [15] Brown GF, Ager JW, Walukiewicz W, Wu J., Sol Energy Mater Sol Cells 2010;94:478-483; <https://doi.org/10.1016/j.solmat.2009.11.010>
- [16] S Singh, Physica Scripta, 2006; 65(2): 167; <https://doi.org/10.1238/Physica.Regular.065a00167>
- [17] A. Merabti, A. Bensliman, H. Issani, S.Nour. Journal of Ovonic Research Vol. 16, No. 5, September -October 2020, p. 261 – 265; <https://doi.org/10.15251/JOR.2020.165.261>
- [18] Tiphaine Galy, Michal Marszewski, Sophia King, Yan Yan, Sarah H. Tolbert, Laurent Pilon, Microporous and Mesoporous Materials Volume 291, 1 January 2020, 109677; <https://doi.org/10.1016/j.micromeso.2019.109677>